# Formability and Damage in Electromagnetically Formed AA5754 and AA6111*

**J.M. Imbert[1], S.L. Winkler[1], M.J. Worswick[1], S. Golovashchenko[2]**

[1] Dept. of Mech. Engineering, University of Waterloo, Waterloo, Ontario, Canada
[2] Ford Motor Company, Scientific Research Laboratory, Dearborn, MI

## Abstract

*This paper presents the results of experiments carried out to determine the formability of AA5754 and AA6111 using electromagnetic forming (EMF), and the effect of the tool/sheet interaction on damage evolution and failure. The experiments consisted of forming 1mm sheets into conical dies of 40° and 45° side angle, using a spiral coil. The experiments showed that both alloys could successfully be formed into the 40° die, with strains above the conventional forming limit diagram (FLD) of both alloys. Forming into the higher 45° cone resulted in failure for both materials. Metallographic analysis indicated that damage is suppressed during the forming process. Micrographs of the necked and fractured areas of the part show evidence that the materials do not fail in pure ductile fracture, but rather in what could be a combination of plastic collapse, ductile fracture and shear band fracture. The failure modes are different for each material; with the AA5754 parts failing by necking and fracture, with significant thinning at the fracture tip. The AA6111 exhibited a saw tooth pattern fractures, a crosshatch pattern of shear bands in the lower half of the part, and tears in the area close to the tip. Both areas showed evidence of shear fracture. This experimental study indicates that there is increased formability for AA5754 and AA6111 when these alloys are formed using EMF. A major factor in this increase in formability is the reduction in damage caused by the tool/sheet interaction.*

## Keywords:

Electromagnetic sheet metal forming, Damage, Formability

---

[*] *Funding from the Ontario Research and Development Challenge fund and Ford Motor Company is gratefully acknowledged. The authors thank V. Dmitriev for helping with the experiments.*

# 1 Introduction

The need to reduce vehicle weight has resulted in increased interest in aluminum alloys for automotive applications. A major factor affecting the application of aluminum alloys in automotive production is their relatively poor formability. This has led to an increased interest in electromagnetic forming (EMF).

Electromagnetic forming has been in use since the late 50's [1]. It has remained a niche manufacturing process mainly used for forming axisymmetric parts with limited sheet applications. Work has recently re-focused on electromagnetic sheet forming techniques. Balenethiram and Daehn [2,3] formed parts using electrohydraulic forming and found a significant increase in formability. Vohnout [4] studied hybrid conventional/EMF operations and found that difficult to form areas in aluminium stampings could be formed using hybrid methods. Oliveira and Worswick [5,6] performed free form and cavity fill EMF experiments with 1.0 and 1.6 mm AA5754 sheet and found increased formability in the cavity fill experiments, but no significant increase in the free form experiments. Golovashenko et al [7] performed electromagnetic and electrohydraulic forming on aluminium sheet and reported an increase of 10-15% in maximum displacement into the die when compared to quasi-static forming. It was also reported that forming into a die could result in increased formability. Recently, the present authors [8,9,10] reported an increase in formability of 1mm AA5754 sheet formed using EMF and proposed that this increase is caused by damage suppression due to the tool/sheet interaction. These conclusions were the result of experimental and numerical analysis of free form and conical (34º side angle) parts formed using a spiral coil. Free-formed samples did not show a significant increase in formability, while the parts formed into a die did.

This paper presents the results of experiments carried out to determine the formability of aluminium alloys AA5754 and AA6111 in an EMF operation, and the effects of the tool/sheet interaction on damage evolution. These alloys were chosen since they are currently used in automotive production. Formability was assessed by forming the alloys into 40 and 45° cones. Strain measurements were taken from the parts using the circle grid technique. Damage and fracture analysis was carried out to determine the effect of the tool/sheet interaction on damage. Optical micrographs showing damage and fracture surfaces are presented.

# 2 Experimental Procedure

## 2.1 Formability Experiments

The experiments consisted of forming 1mm sheet into conical dies of 40° and 45° side angle (100 and 90º included angle) using a spiral coil. A Magnepress [11] system with a maximum storage capacity of 22.5 kJ at 15 kV, capacitance of 200 μF and inductance of 230 nH was used. The conical cavity dies were made from tool steel hardened to 50 Rc. A vacuum port was provided to evacuate the air before each part was formed. Figure 1 shows a schematic of the experimental apparatus.

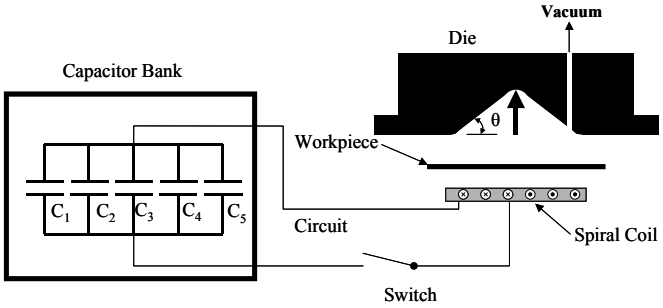


***Figure 1:*** *Schematic of the experimental apparatus*

The material was cut into 165x165 mm (6.5"x 6.5") squares. The AA5754 was provided with a solid film lubricant which was removed. No lubrication was used in the experiments. Circle grids were used to measure the engineering strains. Grids with a nominal diameter of 2.5 mm were applied using electrochemical etching. The strains were measured in the rolling direction using a digital grid measurement system.

### 2.2 Damage Measurements

Metallographic investigations consisted of cold mounting sectioned specimens in epoxy resin, followed by grinding using 320, 600, 1200, and 4000 grit SiC paper and finally polishing using 3 μm and 1 μm diamond paste, and 0.05 μm colloidal silica suspension. 1392 x 1040 pixel, 8-bit grayscale micrographs of the prepared specimens were taken using an Olympus BH2-UMA optical microscope equipped with a Photometrics CoolSNAP CCD camera. A 20x objective lens was employed in combination with white light giving a resolution of 0.729 μm. The images obtained were analyzed using the Image-Pro Plus 5.0 software. The average percent area of voids was determined from void measurements acquired from a minimum of 15 images corresponding to a total analyzed area of approximately 2.0 $mm^2$.

## 3 Results

Safe parts were produced from both alloys with the 40º cone, with charge voltages of 8.0 kV for the AA5754 and 9.0 kV for the AA6111. All the parts formed with the 45º cone failed at charge voltages of 9.0 and 10.0 kV for AA5754 and AA6111, respectively. For the purposes of this work, a part that showed no indication of fracture or necking is considered safe; otherwise it is considered to have failed. Figure 2 and Figure 3 show AA5754 parts formed with the 40 and 45º cones, while Figure 4 and Figure 5 show those formed with AA6111. Three samples for each condition were formed; the ones shown are those that were used for metallographic analysis, unless otherwise noted.

Buckling was observed in all of the formed parts. In the AA5754 samples the buckling is localized in the area of the vacuum hole (Figure 3 B), whereas for AA6111 it was more evenly distributed (Figure 4, Figure 5). Buckling is currently attributed to the indentation produced on the sheet by the vacuum hole. Parts formed in previous experiments with a 34º cone die also showed a distinct indentation, but no buckling [9,10].

The failure modes are different for the two materials studied. AA5754 failed by necking which eventually led to fracture. AA6111 exhibited what appeared to be two distinct types of failure (Figure 5); however, closer examination revealed evidence that both failures were due to shear fracture. Details of the failure will be discussed in section 3.3, below.

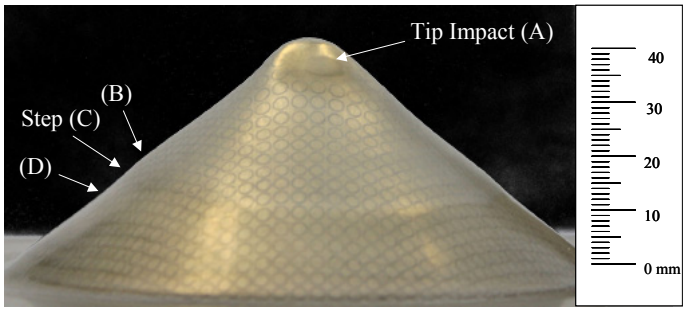


***Figure 2:*** *AA5754 cone formed with the 40° die (8.0 kV)*

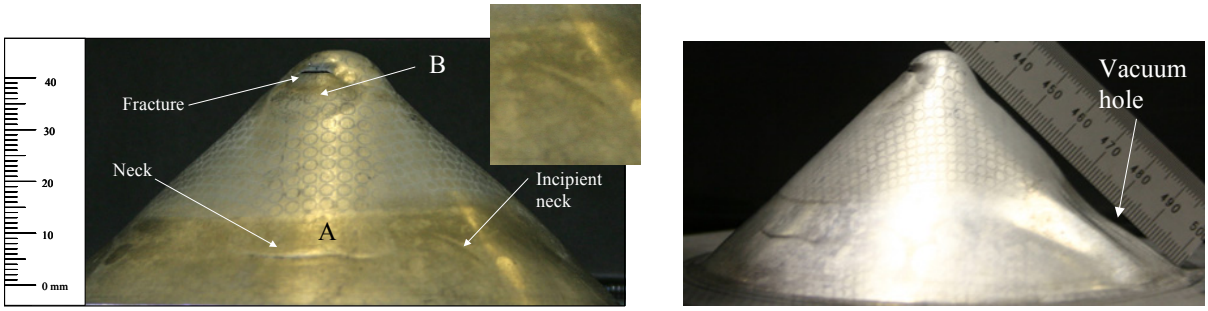


I II

***Figure 3:*** *AA5754 cone formed with the 45° die (9.0 kV). View I shows a neck in the area under the step and fracture near the tip. An incipient neck is shown in the inset. View II shows buckling in the area of the vacuum hole*

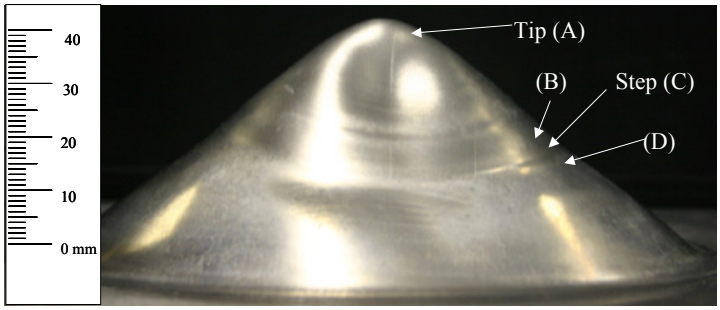


***Figure 4:*** *AA6111 cone formed with the 40° die (9.0 kV). No tip impact was observed in the AA6111 parts*

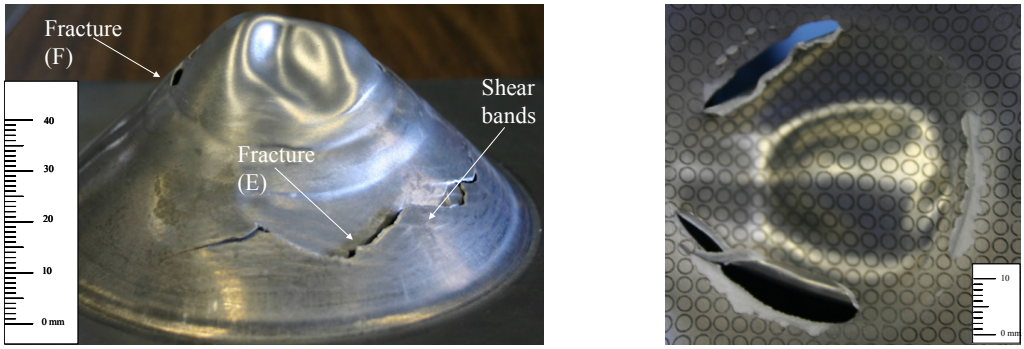


***Figure 5:*** *AA6111 cone formed with the 45° die (10.0 kV). The fracture in the tip area is shown in B (Note that B is from a different sample than the one shown in A). The sample shown in A was used for metallographic analysis*

## 3.1 Formability Data

Figure 6 shows the measured strains for the safe and failed AA5754 parts. Strains above the conventional FLD were observed for the safe parts in the region below the step and the area of tip impact labelled A and D on Figure 2. The data for the failed AA5754 parts also shows very high strains under near plane strain conditions. The highest strains were recorded below the step and below the tip fracture, areas A and B in Figure 3. Figure 7 shows strain measurements for AA5754 samples free-formed with an open cavity die at 6.5 kV charging voltage with the same experimental apparatus [9]. In contrast to the current conical die results; the free-formed samples do not exhibit formability in excess to that obtained using conventional stamping methods.

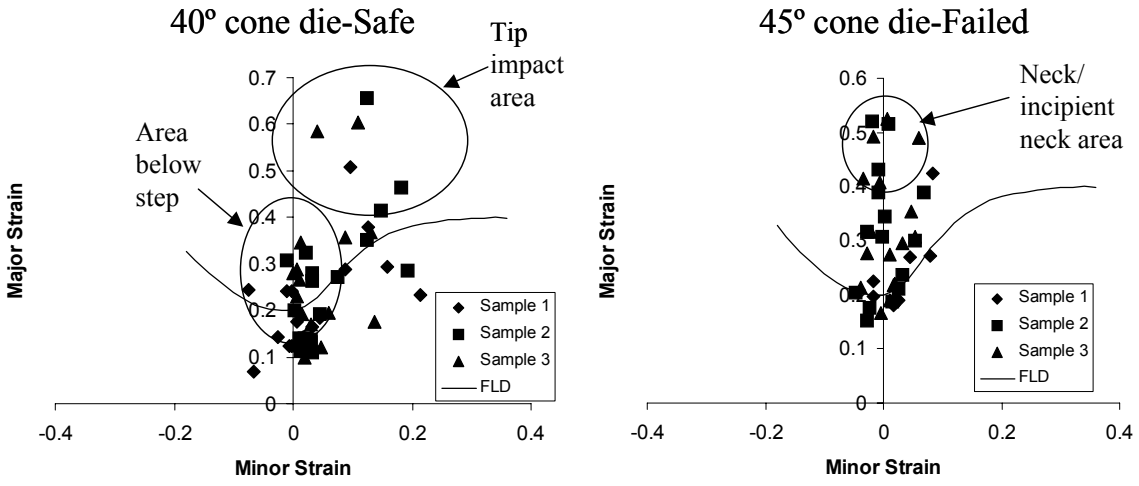


***Figure 6:*** *Strain measurements in FLD format for the safe (left) and failed (right) parts. The curve represents a typical FLD for 1.0 mm AA5754 [12]*

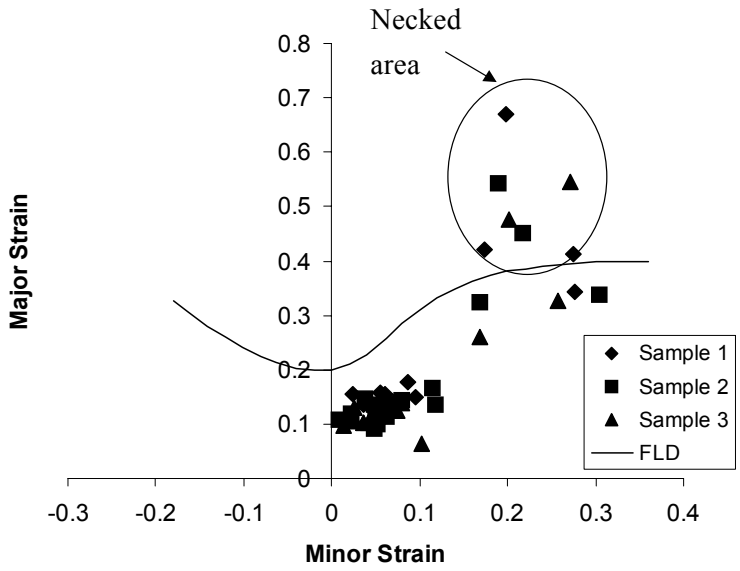


***Figure 7:*** *Strain measurements for necked AA5754 free-formed samples formed using 6.5 kV charge voltage*

Figure 8 shows the strain measurements for the AA6111 safe and failed samples together with a conventional FLD curve. The highest strains were observed below the step for both the safe and failed parts. No impact at the tip of the part occurred, in contrast to the AA5754 parts. Data for the failed samples was taken away from the fracture surface where only incipient necking was present, and in the vicinity of the fracture where the grids were still intact. No strain measurements were taken in the tip region for the failed samples due to the condition of the samples (Figure 5 B). Visual inspection suggests that the strains in this area are significantly lower than the strains presented in Figure 8.

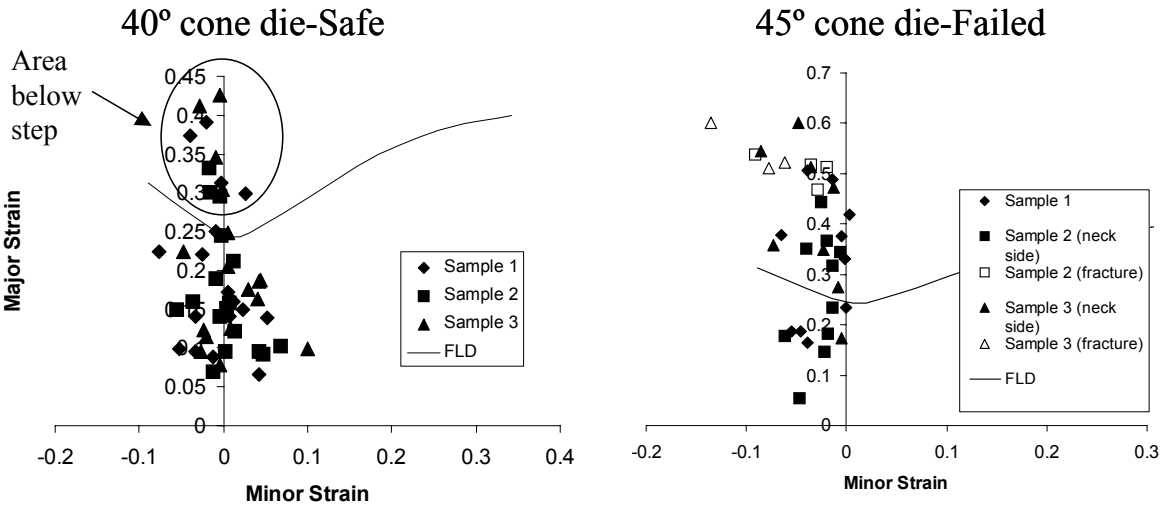


***Figure 8:*** *Strain measurements in FLD format for the safe (left) and failed (right) parts. The curve represents a typical FLD for 0.9 mm AA6111 [12]. No FLD for 1 mm AA6111 sheet was available for publication*

Strains beyond the conventional forming limits were observed for both alloys. In conventional FLD's necking is considered as the forming limit. Using the same criterion the data for the failed samples could be considered as an upper limit of formability for these alloys. The data presented shows an increase in formability for the materials studied. In previous work, the present authors [8,9,10] have postulated that the increase in formability is the result of damage reduction produced by the tool/sheet interaction. The following sections will provide data to support this assertion.

## 3.2 Damage Measurements

Damage measurements are presented in Table 1 for the areas of highest observed damage. The safe parts for both materials exhibit the same damage trends with the highest damage being present in the tip and step areas. Neck measurements were not available for the AA6111, so measurements from the vicinity of the fracture surface are presented.

| **AA5754 as-received data**<br>**Percent area 2nd phase particles = 0.6**<br>**Percent area porosity = 0.010** | | | |
|---|---|---|---|
| Location | Percent area porosity | $e_1$ strain (%) | Condition |
| **40º sample** | | | |
| Tip (A) | 0.067 | 60 | S |
| Above step (B) | 0.011 | 19 | S |
| Step (C) | 0.021 | 22 | S |
| Below step (D) | 0.015 | 26 | S |
| **45º sample** | | | |
| Neck | 0.22 | N/A | N |
| **AA6111 as-received data**<br>**Percent area 2nd phase particles = 0.68**<br>**Percent area porosity = 0.013** | | | |
| **40º sample** | | | |
| Tip (A) | 0.14 | 12 | S |
| Above step (B) | 0.037 | 15 | S |
| Step (C) | 0.081 | 22 | S |
| Below step (D) | 0.05 | 30 | S |
| **45º sample** | | | |
| Fracture (E) | 0.32 | N/A | F |
| Fracture (F) | 0.065 | N/A | F |

***Table 1:*** *Measured porosity for AA5754 and AA6111 samples. The data shown is for safe samples, except for the neck and fracture values. S = safe, N = necked and F = fractured. The locations of regions A-F are shown in Figures 2 to 5*

The formability data and the damage measurements obtained support the damage suppression theory. For AA5754, safe strains beyond the conventional FLD were recorded with the material showing little damage increase relative to the as-received condition, despite the large strains. The data for the cone experiments shows significantly lower dam-

age levels than the ones recorded in the free-formed case for similar strain levels. The area of the neck has an area porosity of 0.15% [9] for major and minor strains of 60% and 20%. This is significantly higher than the 0.067% area porosity for the tip area of the 40º part for major and minor strains of 60% and 10%. Similar data for free-formed AA6111 is currently being obtained.

The highest damage levels for the AA5754 parts were observed in the neck of the failed part, as expected. The fractures in the AA6111 showed two distinct trends, high levels of damage in the saw tooth fracture and relatively little damage in the fractures of the tip region (Figure 5). This is consistent with the higher strains observed in the area of the saw tooth fracture. Both areas show evidence of shear fracture as it will be shown in the following section.

More damage is present in the AA6111, which is consistent with the larger number of second phase particles present in the material, 0.68% area as opposed to 0.60% for AA5754.

### 3.3 Observed Failure

Micrographs of the fracture and necking of the part shown in Figure 3 are shown in Figure 9. It can be seen that the material thinned considerably before fracture in a manner more consistent with plastic collapse than with ductile fracture. The necked area shows voids elongated in the forming direction with significant thinning but relatively little damage. Large voids, similar to the ones present in the neck, could be the precursor to the rectangular feature present in the tip of the fracture surface. The material appears to thin considerably without a corresponding increase in damage. Thinning continues until the voids grow and coalesce to a size where the surrounding areas will either plastically collapse or fail in shear.

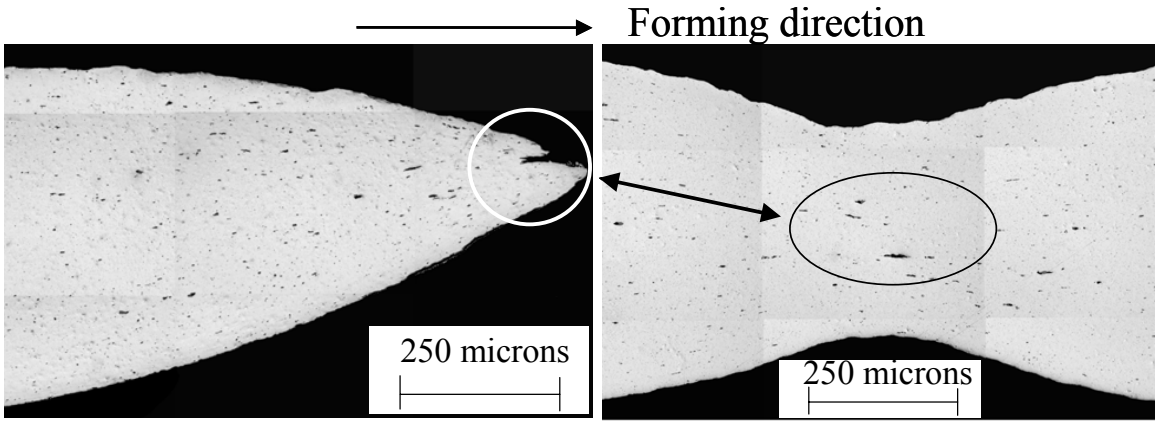


***Figure 9:*** *Micrographs (200x) of the fracture and neck of a AA5754 part formed with the 45° die (Figure 3). Elongated voids, similar to the ones in the centre of the neck, could be the precursor of the rectangular feature present in the tip of the fracture*

Figure 10 shows micrographs of failures observed in AA6111 parts, which are markedly different from the failure observed in AA5754 parts. Both regions show the characteristics of ductile shear failure.

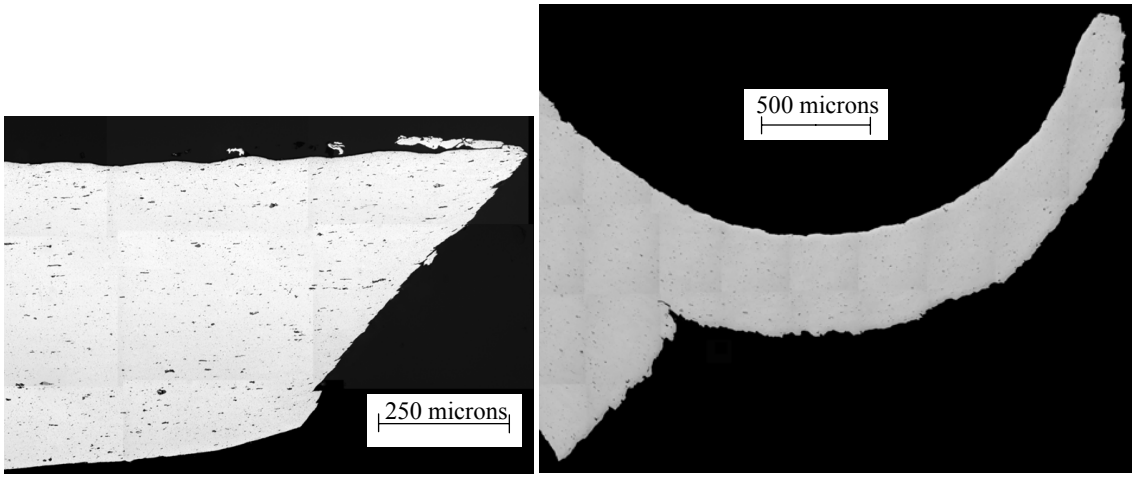


***Figure 10:*** *Micrographs (200x) of the two fracture types observed in AA6111 parts formed with the 45° (Figure 5). Image A corresponds to the saw tooth fracture, while B corresponds to the fracture in the area of the tip (Figure 5)*

The failure modes present in the alloys are consistent with the proposed damage suppression theory during high rate forming. As damage is suppressed, ductile failure gives way to a combination of fracture modes. Although the alloys fail differently, both show evidence of fracture modes other than pure ductile failure. On-going microscopic and scanning electron microscope (SEM) analysis will help to determine the exact nature of the fracture.

## 4 Conclusions

Aluminum alloys AA5754 and AA6111 exhibit increased formability when formed using EMF. The damage measurements obtained support the theory that this increase is due to the suppression of damage caused by the tool/sheet interaction. The materials do not fail in pure ductile failure; rather, the failure modes seem to be a combination of plastic collapse, ductile failure, and shear localization. The failure modes for AA5754 and AA6111 in EMF are significantly different with the former showing significant thinning prior to fracture and evidence of what could be a combination of plastic collapse and ductile fracture, while the latter shows clear evidence of shear fracture. The vacuum hole has a significant effect on the quality of the formed parts, and its geometry and positioning are important considerations when designing EMF dies.

## References

[1] *Wagner, H.J. and Boulger, F.W.:* High Velocity Metalworking Processes Based on the Sudden Release of Electrical of Electrical Energy. Memorandum prepared by the Battle Memorial Institute for the Defense Metals Information Center, 1960.

[2] *Balanethiram, V.S. and Daehn, G.S.:* Hyperplasticity: Increased Forming Limits at High Workpiece Velocity. Scripta Metall. et Mater., 30, 1994 pp. 515-520.

[3] *Balanethiram, V.S.:* Hyperplasticity: Enhanced Formability of Sheet Metals at High Workpiece Velocities. Ph.D. Thesis, The Ohio State University, 1996.

[4] *Vohnout, V.S.:* A Hybrid Quasi-Static/Dynamic Process for Forming Large Sheet Metal Parts From Aluminum Alloys. Ph.D. thesis, The Ohio State University, 1998.

[5] *Oliveira, D.A.:* Electromagnetic Forming of Aluminum Alloy Sheet: Experiment and Model. Masters of Applied Science thesis, University of Waterloo, 2002.

[6] *Oliveira, D.A. and Worswick, M.J.:* Electromagnetic Forming of Aluminum Alloy Sheet. J. Phys. IV France 110, EDP Sciences, Les Ulis, DOI: 10.1051/jp4:20030709, 2003, pp. 293-298.

[7] *Golovashchenko, S.:* Numerical and Experimental Results on Pulsed Tube Calibration. Proceedings of the TMS annual meeting “Sheet metal forming technology, M. Demeri ed., San Diego, Ca., 1999, pp. 117-127.

[8] *Imbert, J.M., Winkler, S.L., Worswick, M.J., Oliveira, D.A. and Golovashchenko, S.:* Damage Prediction in Aluminum Alloy Sheet Electromagnetic Forming. Proceedings of Plasticity’03 “The Tenth International Symposium on Plasticity and its Current Applications”, A. Khan ed., Quebec City, 2003, pp. 178-180.

[9] *Imbert, J.M., Winkler, S.L., Worswick, M.J., Oliveira, D.A. and Golovashchenko, S.:* The Effect of Tool/Sheet Interaction on Damage Evolution in Electromagnetic Forming of Aluminum Alloy Sheet. Submitted for publication, Dec. 2003.

[10] *Imbert, J.M., Winkler, S.L., Worswick, M.J., Oliveira, D.A. and Golovashchenko, S.:*Numerical Study of Damage Evolution and Failure in an Electromagnetic Corner Fill Operation. Proceedings of NUMIFORM04, Columbus, Ohio, June 2004. To be published.

[11] IAP Research Inc. 2003. Magnepress System product information. http://www.iap.com/2col.html.

[12] Data provided by Alcan *International.*